

**Chiu et al. “Diverse cellular morphologies during lumen maturation in *Anopheles gambiae* larval salivary glands”.**

**Supplementary Figure Legends**

**Figure S1. Morphological characterization and cell count in an L4.2 salivary gland.**

(A-B,G) Representative images of L4 SGs stained with Hoechst (DNA, purple) and Nile Red (lipids, blue) dyes. (A-B) SG regions are outlined with a yellow dashed line. (A,D-E) Colored arrows (green, duct bud; yellow, small; orange, medium; blue, large) correspond to the size category of that cell and nucleus. (A) Cells and nuclei were counted in each L4 SG region and cells were classified into one of four discrete size categories (see D, E). The white arrows in (iii) indicate, from top to bottom: the duct bud region, the duct bud-proximal sac interface, and the proximal sac region. (B) An L4 SG showcasing the variety of cell/DNA sizes and shapes observed. Very small cells are marked by white arrows, while small, medium, and large cells are shown in (iv), (v), and (vi). (C) L4 SG length measurements by region. (D-E) In this L4 SG, there were 300 duct bud cells, 20 proximal sac cells, and 80 distal sac cells. Cell and DNA measurements are shown for the duct bud (D), the proximal sac (E), and the distal sac (E). (F) L4 SG proximal and distal sacs are connected by a single, shared lumen. Yellow arrows (i) indicate apical domains enriched for lipids and cytoplasmic markers (mtTFA, lamin). A row of cells (ii-iii) defines the boundary between PS and DS regions (white arrows, ii-iii). The lumen narrows slightly between sacs (white arrows, iv-v).

**Figure S2. Paucity of cells positive for two markers of Notch signaling.** Representative images from L4 SGs stained with Hoechst (DNA, purple), Nile Red (lipids, blue) and antisera against either Delta (green, A) or Notch (green, B). (A) Only three sac or duct bud cells with Delta staining (arrows). (B) No cells positive for Notch (B) in any larval SG region.

**Figure S3. Multiple control analyses strongly indicate high robustness of our staining methodology.** Various control and validation dye- and immuno-staining and confocal microscopy results in support of our methodology. (A) Representative images from L4 *Anopheles gambiae* salivary glands (SGs) stained with no primary antisera and only the secondary antibodies goat anti-mouse 647 (purple) and goat anti-rabbit 488 (green; i) or goat anti-rat 647 (purple) and donkey anti-goat 488 (green; ii). DIC light microscopy (not shown) allowed us to outline the SGs (dashed yellow line), and the fluorescence settings used were consistent with those used for SG staining throughout the study. (B-K) Representative images from L4 *Anopheles gambiae* salivary glands (SGs) stained with the dyes DAPI (DNA, purple), Nile Red (lipids, blue), and antisera against Fibrillarin (nucleolus; B; white), GM130 (Golgi; B; green), Cad99c (apical polarity marker; C; green), H+ V-ATPase (apical polarity marker; D; green), or Na+/K+ ATPase (apical polarity marker; E; green). (B) Pre-clearing various antisera using 0-2 hour old *Drosophila melanogaster* embryos did not alter the broad patterns of staining observed. Nucleoli (yellow arrows, B), basement membrane signal (yellow arrows, C) and cytoplasmic signal (yellow asterisks) are visible (compare Figs. S1B, 3C, and 3D). (C-E) Polarity marker localizations were confirmed in gastric cecae (white arrows, asterisks; Dii, Ev-vii), then determined in larval SG cells. Basement membrane localization (yellow arrows) and cytoplasmic signal (yellow asterisks) were observed. Very faint nuclear and nuclear membrane signal (Figs. S1Eiii-iv, orange and red arrows, respectively) were visible. (F) Representative images from day seven adult *Anopheles gambiae* female SGs permeablized with cold acetone and stained with DAPI

(DNA) and anti-lamin antisera. Results show variable nuclear shape persists at this stage and lamin C typically shows complete coverage of the perinuclear region in all cells. PL-proximal lateral lobe; DL-distal lateral lobe; M-medial lobe.

**Figure S4. Control analyses of *Drosophila* salivary gland TF antisera confirm that the staining methodology and reagents perform well.** Various control and validation dye- and immuno-staining and confocal microscopy results in support of our methodology. (A-F) Representative images from L4 *Anopheles gambiae* salivary glands (SGs) stained with the dyes DAPI (DNA, purple), Nile Red (lipids, blue), and stained with antibodies against CrebA (SG TF; A, C, E; green/white), Sage (SG TF; B, D, F; green/white), CrebA pre-IgG serum (D; green), or Sage pre-IgG serum (C; green). (A) CrebA antisera raised in two different host species colocalize (yellow arrows) on DNA and in SG cells. (B) Pre-clearing various antisera using 0-2 hour old *Drosophila melanogaster* embryos did not alter the broad patterns of staining observed (compare Figs. S2B, 3A, and 4A/D). Nucleoli, basement membrane signal (yellow arrows) and cytoplasmic signal (yellow asterisks) are visible. (C-D) Staining with Sage (C) or CrebA (D) pre-IgG serum did not show appreciable signal. (E-F) Staining with either CrebA (E) or Sage (F) showed very little, or no, localization to gastric cecae DNA.

**Figure S5. DAVID Results Contributing to GO Terms of Interest List and Extended Larval Anatomy Gene Expression Comparison.** (A) Tables showing the top 10 functional categories for each sector of the Venn Diagram shown in Figure 6A. These tables were used to define the GO categories of interest list (black text) in Figure 6D. (B) An extended version of Table 6C that includes expressed gene comparisons between larval gut compartments.

**Figure S6. Gene Lists Resulting from, and Experimental Evidence in Support of, the Gene Expression Meta-Analysis.** (A) List of all 496 genes expressed in every experiment included (Table S1) in gene expression meta-analysis, listed either by Vectorbase common name (57 genes) or Vectorbase ID (439 genes). (B) List of all 86 genes expressed only in larval SGs with respect to all datasets (Table S1) in this gene expression meta-analysis. (C) Reverse-transcriptase PCR from one representative technical replicate across five biological replicates of *Anopheles gambiae* (G3 strain) L4 stage SG, GC, or midgut replicates, amplifying two control genes (actin and elongation factor), as well as three SG transcription factors (*CrebA*, *fkh*, and *sage*), two saliva proteins important for adult blood feeding (*SG6* and *saglin*), and three digestive enzymes (*5' nucleosidase*, *maltase*, and *peroxidase*). All genes are expressed in all tissues (to widely varying levels), but not in all samples – except for *sage*, which is not observed in midgut samples. (D) Quantitative reverse transcriptase PCR abundance values [ $2^{-\Delta\Delta C_T}$ ] for the same set of samples and genes described in (C), with all five replicates averaged. In all cases except *sage* in midguts, again, all genes are expressed in all tissues to some level.

Figure S1

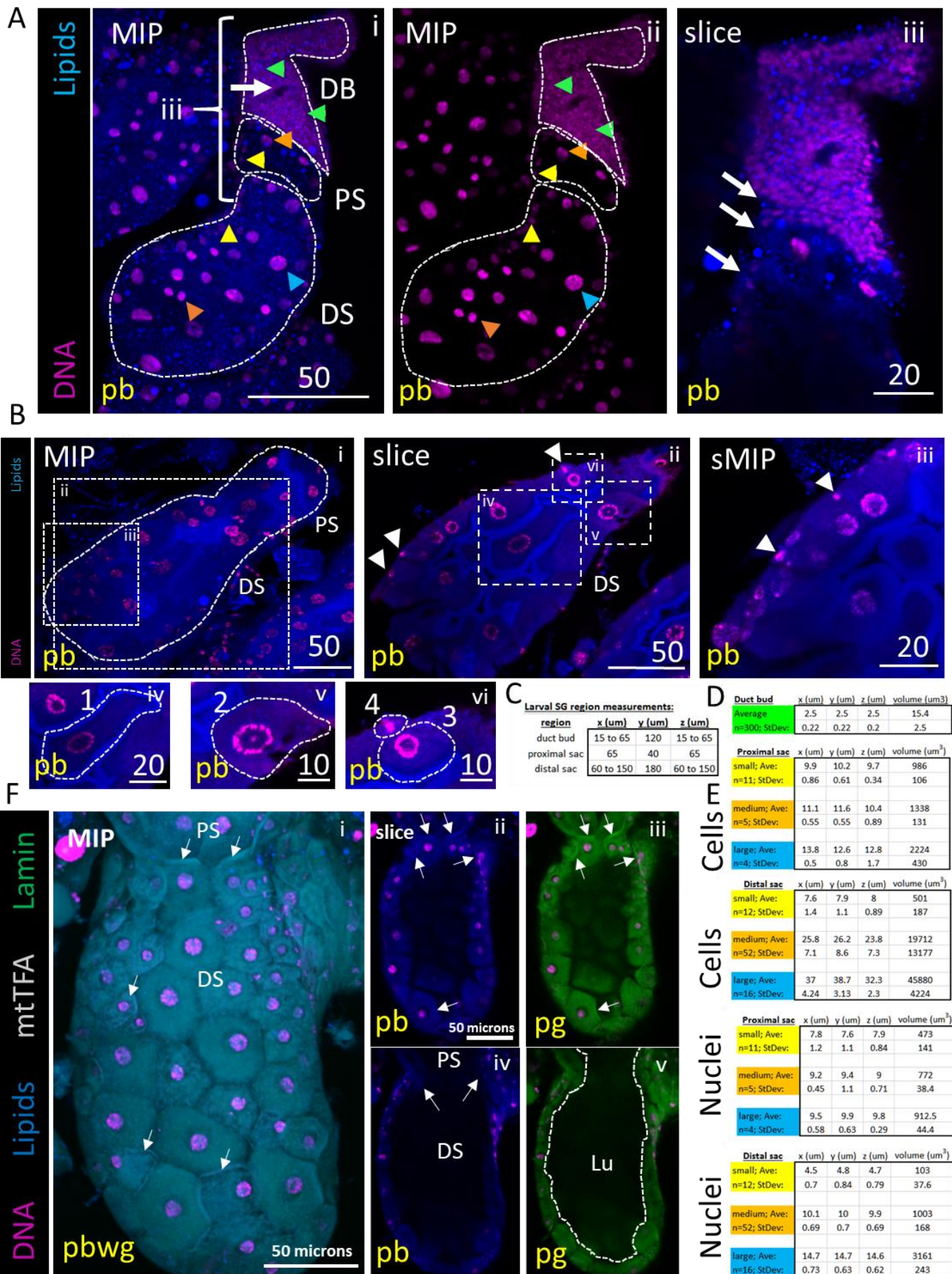


Figure S2

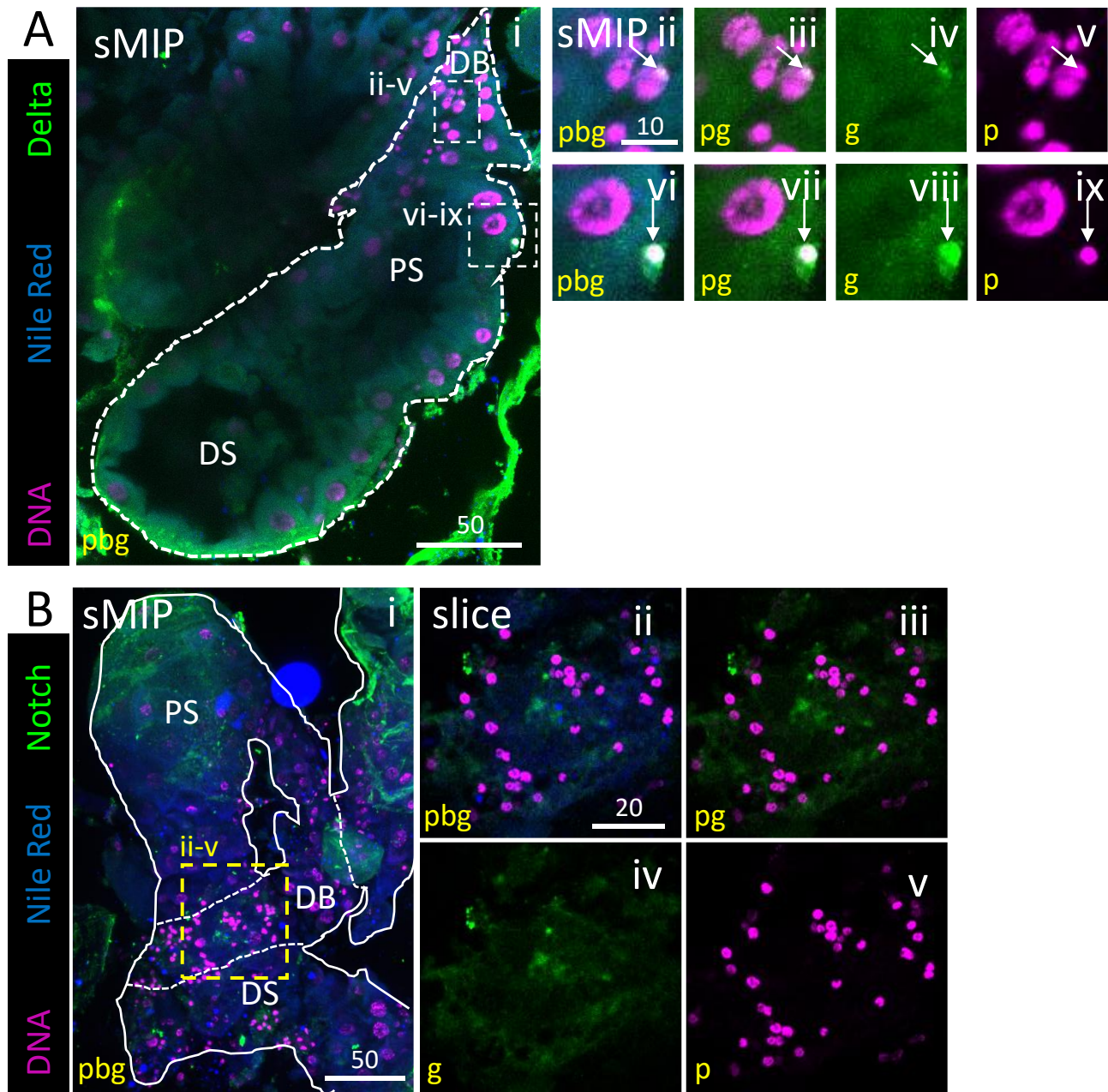


Figure S3

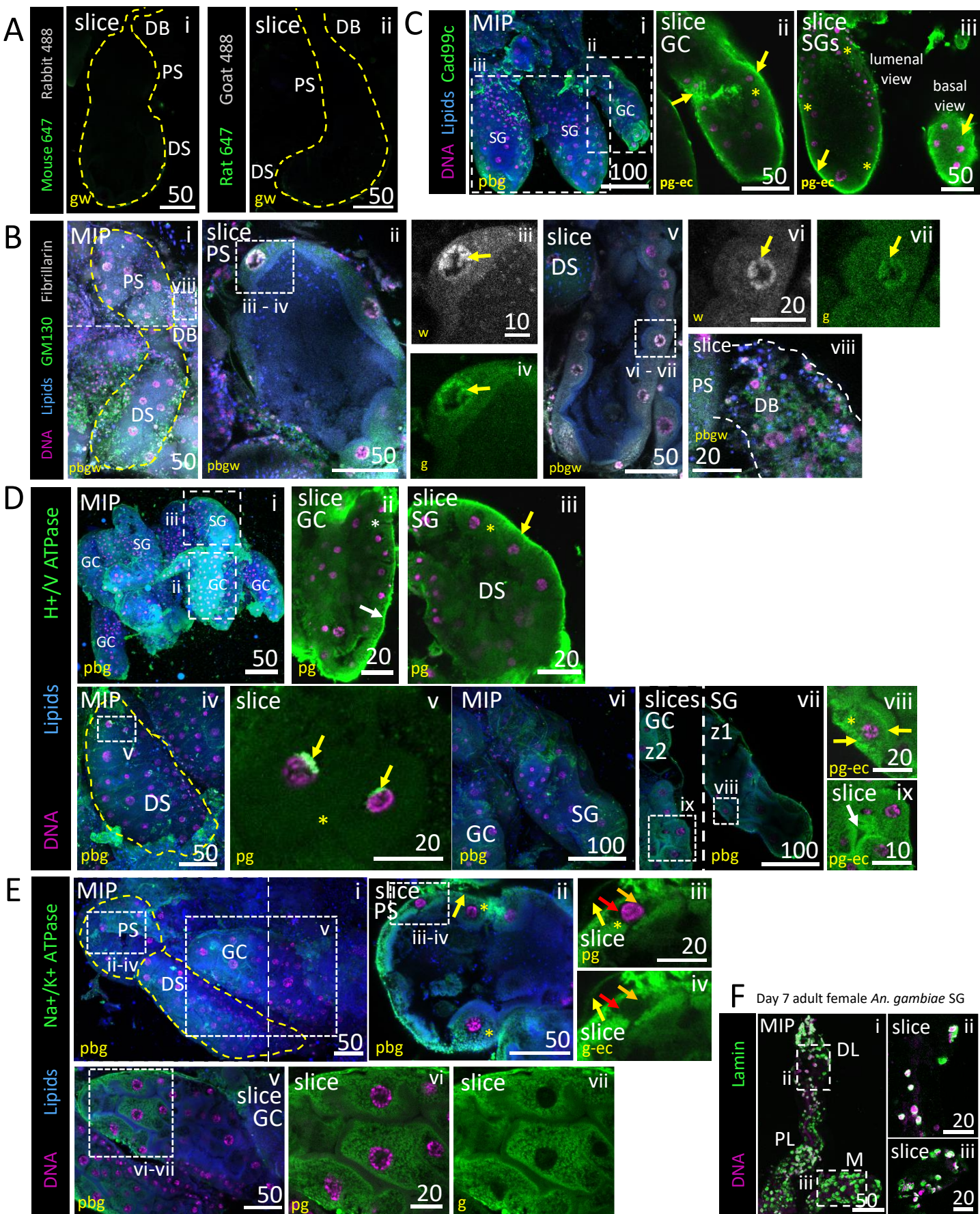
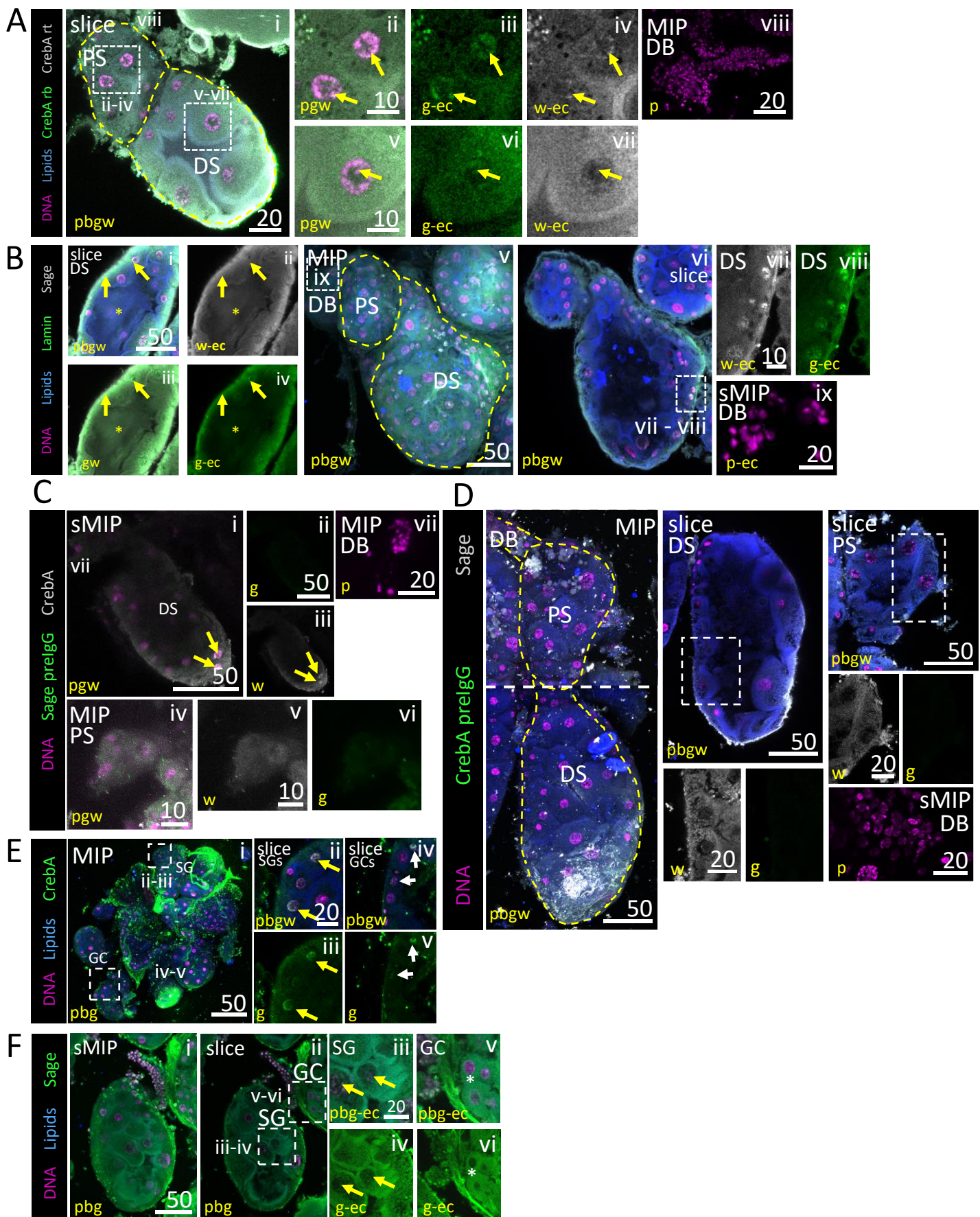


Figure S4



**Table S1. Gene expression datasets analyzed in this study.**

<b>Tissue</b>	<b>Stage</b>	<b>Species</b>	<b>Sex</b>	<b>Assay</b>	<b>NCBI GEO/SRA Accession Number(s)</b>
Salivary Gland	L4 larvae	<i>Anopheles gambiae</i>	mixed	microarray	GSM243576-GSM243578
Salivary Gland	Adult	<i>Anopheles gambiae</i>	female	microarray	GSM541203-GSM541206
Salivary Gland	Adult	<i>Anopheles gambiae</i>	male	microarray	GSM541207-GSM541210
Gastric Cecae	L4 larvae	<i>Anopheles gambiae</i>	mixed	microarray	GSM172187-GSM172189
Larval Anterior Midgut	L4 larvae	<i>Anopheles gambiae</i>	mixed	microarray	GSM172190-GSM172192
Larval Posterior Midgut	L4 larvae	<i>Anopheles gambiae</i>	mixed	microarray	GSM172193-GSM172195
Larval Hindgut	L4 larvae	<i>Anopheles gambiae</i>	mixed	microarray	GSM172196-GSM172198
Midgut	Adult	<i>Anopheles gambiae</i>	female	microarray	GSM541191-GSM541194
Midgut	Adult	<i>Anopheles gambiae</i>	male	microarray	GSM541195-GSM541198
Ovary	Adult	<i>Anopheles gambiae</i>	female	microarray	GSM541199-GSM541202
Testes	Adult	<i>Anopheles gambiae</i>	male	microarray	GSM541211-GSM541214

**Table S2. 474 Unique Vectorbase ID's of Combined Genes Resulting from DAVID Results of Meta-Analysis and Salivary Gland Genes of Interest Lists.**

Vectorbase ID
AGAP000029
AGAP000035
AGAP000044
AGAP000047
AGAP000150
AGAP000151
AGAP000152
AGAP000187
AGAP000198
AGAP000240
AGAP000374
AGAP000376
AGAP000426
AGAP000436
AGAP000541
AGAP000548
AGAP000561
AGAP000597
AGAP000607
AGAP000609
AGAP000610
AGAP000611
AGAP000612
AGAP000623
AGAP000646
AGAP000651
AGAP000654
AGAP000655
AGAP000728
AGAP000739
AGAP000747
AGAP000751
AGAP000776
AGAP000830
AGAP000898
AGAP000927
AGAP000930
AGAP000949
AGAP000953
AGAP001015
AGAP001043
AGAP001053
AGAP001093
AGAP001194
AGAP001198
AGAP001218
AGAP001219
AGAP001274
AGAP001322
AGAP001326
AGAP001335
AGAP001335
AGAP001374
AGAP001376
AGAP001414
AGAP001459
AGAP001464
AGAP001539
AGAP001545
AGAP001570
AGAP001595
AGAP001671
AGAP001676
AGAP003004
AGAP004886
AGAP006522
AGAP008306
AGAP010252
AGAP011842
AGAP003025
AGAP004887
AGAP006612
AGAP008307
AGAP010257
AGAP011849
AGAP003069
AGAP004919
AGAP006614
AGAP008329
AGAP010261
AGAP011896
AGAP003147
AGAP004920
AGAP006625
AGAP008339
AGAP010265
AGAP011902
AGAP003183
AGAP004921
AGAP006632
AGAP008341
AGAP010286
AGAP011912
AGAP003230
AGAP004922
AGAP006686
AGAP008362
AGAP010313
AGAP011913
AGAP003301
AGAP004957
AGAP006688
AGAP008440
AGAP010386
AGAP011914
AGAP003354
AGAP004989
AGAP006771
AGAP008532
AGAP010396
AGAP011938
AGAP003412
AGAP005003
AGAP006797
AGAP008560
AGAP010406
AGAP011951
AGAP003473
AGAP005046
AGAP006871
AGAP008566
AGAP010510
AGAP011961
AGAP003474
AGAP005061
AGAP006879
AGAP008622
AGAP010591
AGAP011970
AGAP003488
AGAP005095
AGAP006895
AGAP008623
AGAP010592
AGAP011971
AGAP003532
AGAP005110
AGAP006898
AGAP008687
AGAP010629
AGAP011996
AGAP003538
AGAP005131
AGAP007157
AGAP008726
AGAP010647
AGAP012013
AGAP003553
AGAP005176
AGAP007258
AGAP008819
AGAP010655
AGAP012014
AGAP003556
AGAP005213
AGAP007327
AGAP008875
AGAP010719
AGAP012056
AGAP003560
AGAP005222
AGAP007361
AGAP008896
AGAP010735
AGAP012077
AGAP003592
AGAP005263
AGAP007381
AGAP008906
AGAP010736
AGAP012100
AGAP003618
AGAP005317
AGAP007393
AGAP008908
AGAP010784
AGAP012111
AGAP003676
AGAP005318
AGAP007474
AGAP008916
AGAP010828
AGAP012138
AGAP003681
AGAP005319
AGAP007492
AGAP009022
AGAP010894
AGAP012211
AGAP003703
AGAP005337
AGAP007502
AGAP009031
AGAP010895
AGAP012229
AGAP003738
AGAP005339
AGAP007523
AGAP009049
AGAP010921
AGAP012284
AGAP003768
AGAP005427
AGAP007532
AGAP009182
AGAP010926
AGAP012305
AGAP003816
AGAP005469
AGAP007540
AGAP009207
AGAP010929
AGAP012407
AGAP003824
AGAP005520
AGAP007543
AGAP009324
AGAP010933
AGAP012464
AGAP003899
AGAP005575
AGAP007580
AGAP009338
AGAP010985
AGAP012521
AGAP003902
AGAP005578
AGAP007581
AGAP009431
AGAP011026
AGAP012603
AGAP003967
AGAP005609
AGAP007586
AGAP009460
AGAP011033
AGAP012633
AGAP003970
AGAP005634
AGAP007635
AGAP009461
AGAP011038
AGAP012755
AGAP003975
AGAP005802
AGAP007644
AGAP009483
AGAP011077
AGAP012756
AGAP003984
AGAP005817
AGAP007650
AGAP009503
AGAP011162
AGAP012798
AGAP004050
AGAP005822
AGAP007690
AGAP009508
AGAP011173
AGAP012879
AGAP004098
AGAP005839
AGAP007706
AGAP009537
AGAP011203
AGAP012890
AGAP004192
AGAP005853
AGAP007709
AGAP009554
AGAP011214
AGAP012906
AGAP004194
AGAP005857
AGAP007740
AGAP009572
AGAP011246
AGAP012990
AGAP004211
AGAP005930
AGAP007797
AGAP009632
AGAP011298
AGAP012991
AGAP004212
AGAP005947
AGAP007826
AGAP009730
AGAP011354
AGAP013120
AGAP004239
AGAP005960
AGAP007831
AGAP009748
AGAP011358
AGAP013166
AGAP004275
AGAP005991
AGAP007834
AGAP009784
AGAP011359
AGAP013192
AGAP004296
AGAP006037
AGAP007864
AGAP009861
AGAP011396
AGAP013260
AGAP004334
AGAP006044
AGAP007913
AGAP009880
AGAP011402
AGAP013266
AGAP004335
AGAP006086
AGAP007927
AGAP009910
AGAP011424
AGAP013335
AGAP004422
AGAP006141
AGAP007940
AGAP009917
AGAP011448
AGAP013423
AGAP004439
AGAP006371
AGAP008015
AGAP009920
AGAP011501
AGAP013516
AGAP004488
AGAP006386
AGAP008044
AGAP009942
AGAP011504
AGAP013724
AGAP004494
AGAP006388
AGAP008060
AGAP009948
AGAP011514
AGAP013742
AGAP004560
AGAP006414
AGAP008061
AGAP009974
AGAP011515
AGAP028120
AGAP004579
AGAP006418
AGAP008118
AGAP009998
AGAP011516
AGAP028125
AGAP004625
AGAP006419
AGAP008191
AGAP010010
AGAP011551
AGAP028143
AGAP004628
AGAP006420
AGAP008215
AGAP010017
AGAP011552
AGAP028694
AGAP004699
AGAP006421
AGAP008216
AGAP010065
AGAP011687
AGAP029544
AGAP004743
AGAP006462
AGAP008278
AGAP010160
AGAP011691
AGAP004754
AGAP006477
AGAP008279
AGAP010163
AGAP011693
AGAP004798
AGAP006494
AGAP008280
AGAP010216
AGAP011706
AGAP004819
AGAP006495
AGAP008281
AGAP010220
AGAP011725
AGAP004831
AGAP006504
AGAP008282
AGAP010224
AGAP011777
AGAP004852
AGAP006506
AGAP008283
AGAP010225
AGAP011799
AGAP004876
AGAP006511
AGAP008284
AGAP010251
AGAP011802



# Figure S5

## A

**i**

Larvae: GO Term	Gene Count	%	P-Value	Benjamini
transporter activity	12	1.7	4.00E-03	7.10E-01
retrograde vesicle-mediated transport, Golgi to ER	5	0.7	6.90E-03	9.30E-01
endoplasmic reticulum	11	1.6	9.80E-03	7.90E-01
pyrimidine nucleotide biosynthetic process	3	0.4	1.10E-02	8.80E-01
mitophagy	5	0.7	1.90E-02	9.10E-01
phospholipid-translocating ATPase activity	3	0.4	3.20E-02	9.90E-01
CCR4-NOT core complex	3	0.4	3.20E-02	9.30E-01
protein localization to pre-autophagosomal structure	3	0.4	3.50E-02	9.60E-01
ceramide biosynthetic process	3	0.4	3.50E-02	9.60E-01
nucleophagy	4	0.6	3.50E-02	9.30E-01

**ii**

Female: GO Term	Gene Count	%	P-Value	Benjamini
transaminase activity	3	0.4	2.40E-02	1.00E+00
nucleosomal DNA binding	4	0.5	2.50E-02	9.80E-01
iron-sulfur cluster binding	4	0.5	2.50E-02	9.80E-01
lipid transporter activity	4	0.5	3.20E-02	9.70E-01
cytoplasmic microtubule organization	4	0.5	3.60E-02	1.00E+00
cell division	4	0.5	3.60E-02	1.00E+00
ATPase activity, coupled to transmembrane movement of substances	7	1	3.80E-02	9.50E-01
3-oxo-lignoceronyl-CoA synthase activity	5	0.7	4.00E-02	9.20E-01
3-oxo-arachidoyl-CoA synthase activity	5	0.7	4.00E-02	9.20E-01
3-oxo-cerotoyl-CoA synthase activity	5	0.7	4.00E-02	9.20E-01

**iii**

Male: GO Term	Gene Count	%	P-Value	Benjamini
dynein complex	7	1.2	2.70E-05	2.70E-03
integral component of plasma membrane	31	5.1	5.30E-05	2.60E-03
1-acylglycerol-3-phosphate O-acyltransferase activity	5	0.8	3.90E-04	8.70E-02
microtubule motor activity	8	1.3	1.30E-03	1.40E-01
histone H3-K4 methylation	4	0.7	2.20E-03	4.50E-01
microtubule-based movement	8	1.3	2.40E-03	2.80E-01
sensory perception of smell	6	1	2.50E-03	2.00E-01
iron ion binding	18	3	2.60E-03	1.80E-01
monooxygenase activity	14	2.3	2.80E-03	1.50E-01
oxidoreductase activity	18	3	4.30E-03	1.80E-01

**iv**

L&M: GO Term	Gene Count	%	P-Value	Benjamini
heme binding	7	4.2	1.90E-02	8.80E-01
oxidoreductase activity, acting on paired donors, with incorporation or reduction of molecular oxygen	6	3.6	2.20E-02	6.90E-01
signal transducer activity	3	1.8	4.60E-02	8.10E-01
hexose transmembrane transport	3	1.8	5.20E-02	1.00E+00
glucose import	3	1.8	5.20E-02	1.00E+00
glucose transmembrane transporter activity	3	1.8	5.20E-02	7.60E-01
triglyceride biosynthetic process	2	1.2	5.40E-02	9.40E-01
protein glycosylation	3	1.8	5.90E-02	8.80E-01
sugar:proton symporter activity	3	1.8	6.30E-02	7.50E-01
iron ion binding	6	3.6	6.60E-02	7.00E-01

**v**

L&F: GO Term	Gene Count	%	P-Value	Benjamini
response to stress	5	1.3	1.60E-04	3.70E-02
protein folding	11	2.8	2.20E-04	2.60E-02
ATP binding	39	10	7.00E-04	1.20E-01
GTP binding	13	3.3	2.00E-03	1.60E-01
endoplasmic reticulum	9	2.3	2.30E-03	2.40E-01
endosome	5	1.3	3.80E-03	2.00E-01
U1 snRNP	4	1	8.20E-03	2.80E-01
tRNA modification	3	0.8	3.70E-02	9.50E-01
response to endoplasmic reticulum stress	3	0.8	4.60E-02	9.40E-01
isoprenoid biosynthetic process	3	0.8	4.60E-02	9.40E-01

**vi**

M&F: GO Term	Gene Count	%	P-Value	Benjamini
oxidoreductase activity	39	2.9	4.00E-05	1.90E-02
proteolysis	17	1.3	4.90E-04	2.50E-01
digestion	7	0.5	9.80E-04	2.50E-01
catalytic activity	22	1.6	7.70E-03	8.50E-01
N-acetylmuramoyl-L-alanine amidase activity	5	0.4	9.30E-03	7.80E-01
peptidoglycan catabolic process	5	0.4	1.10E-02	8.90E-01
RNA processing	9	0.7	1.80E-02	9.30E-01
methyltransferase activity	7	0.5	1.90E-02	9.00E-01
nuclear nucleosome	4	0.3	2.10E-02	9.90E-01
serine-type carboxypeptidase activity	6	0.4	3.30E-02	9.60E-01

**vii**

ALL: GO Term	Gene Count	%	P-Value	Benjamini
structural constituent of ribosome	137	4.9	3.00E-47	2.40E-44
translation	112	4	1.60E-26	1.70E-23
cytosolic large ribosomal subunit	49	1.7	2.00E-23	8.10E-21
cytosolic small ribosomal subunit	32	1.1	2.00E-15	4.10E-13
mitochondrion	103	3.7	3.50E-14	4.80E-12
ribosome	26	0.9	3.00E-12	3.00E-10
RNA binding	84	3	3.00E-10	1.20E-07
protein folding	48	1.7	4.50E-09	2.30E-06
translation initiation factor activity	23	0.8	1.40E-08	3.80E-06
cytoplasm	252	9	5.70E-08	4.70E-06

**viii**

NONE: GO Term	Gene Count	%	P-Value	Benjamini
plasma membrane	229	4.3	5.60E-22	2.30E-19
olfactory receptor activity	112	2.1	2.20E-21	1.80E-18
detection of the chemical stimulus involved in sensory perception of smell	67	1.3	1.10E-17	1.30E-14
nucleus	527	9.9	3.80E-16	6.90E-14
odorant binding	119	2.2	1.00E-15	4.10E-13
sequence-specific DNA binding	128	2.4	3.10E-15	8.10E-13
regulation of transcription, DNA-templated	135	2.5	5.70E-14	3.10E-11
signal transduction	91	1.7	4.90E-10	1.80E-07
transcription factor activity, sequence-specific DNA binding	102	1.9	6.00E-09	1.20E-06
zinc ion binding	325	6.1	7.40E-08	1.20E-05

## B

Comparison	Stage	SG Present	Tissue Present	SG present	Absent
		Tissue Absent	SG Absent	Tissue Present	in Both
Gastric Cecae vs. Anterior Midgut	Larval	54% (3672)	25% (1734)	21% (1407)	5779
Gastric Cecae vs. Posterior Midgut	Larval	45% (3271)	30% (2206)	35% (1808)	5307
Gastric cecae vs. Hindgut	Larval	28% (2338)	39% (3294)	33% (2741)	4219
Anterior Midgut vs. Posterior Midgut	Larval	4% (188)	25% (1061)	70% (2953)	8390
Anterior Midgut vs. Hindgut	Larval	2% (133)	49% (3027)	49% (3008)	6424
Posterior Midgut vs. Hindgut	Larval	3% (209)	36% (2230)	61% (3805)	6348
SG vs. Gastric Cecae	Larval	10.3% (582)	31.4% (1778)	<b>58.3% (3301)</b>	6931
SG vs. Anterior Midgut	Larval	<b>47.2% (2804)</b>	34.7% (2062)	18.1% (1079)	6647
SG vs. Posterior Midgut	Larval	<b>38.4% (2498)</b>	40.4% (2629)	21.3% (1385)	6080
SG vs. Hindgut	Larval	23.2% (1819)	<b>50.6% (3971)</b>	26.3% (2064)	4738
SG vs. Midgut (Female)	Adult	21.8% (1296)	18% (1069)	<b>60.3% (3588)</b>	6639
SG vs. Midgut (Male)	Adult	19.7% (1144)	19.3% (1123)	<b>60.9% (3538)</b>	6787
SG vs. Ovary	Adult	27.5% (1999)	<b>46.4% (3377)</b>	26% (1884)	5332
SG vs. Testes	Adult	20.2% (1676)	<b>53.2% (4420)</b>	26.6% (2207)	4291



**Table S3. Primers used for Independent Validation by RT-PCR and RT-qPCR Analysis of Controls and a Subset of Meta-Analysis Genes.**

Gene	Primer ID	Sequence	Product size
Forkhead: AGAP001671	Fkh_f 262730040	5'- CATGGATCTGTTCCCGTTCT-3'	220 bp
	Fkh_r 262730041	5'- CACCTCCTTCTTCTCGTCCTT-3'	
CrebA: AGAP011038	CrebA_f 262730048	5'- GACGTGACATGGAGGAGAT-3'	200 bp
	CrebA_r 262730049	5'- GTACTCCTTCTTGCGCTTGC -3'	
Apyrase: AGAP011971	Apy_f 262730060	5'- GGGTGACAACCTCCAGGGTA -3'	300 bp
	Apy_r 262730061	5'- TAGAGCGGATCAGGTTGTC -3'	
5' Nucleosidase: AGAP011026	5nucleo_f 262730064	5'- CTGCGCTTAAGAAGGACCAG -3'	200 bp
	5nucleo_r 262730065	5'- TACCGTTGGTGTGGTTCTCA -3'	
Maltase: AGAP002102	Mal_f 262730074	5'- GCTGCTGACGGTGAACAGTA -3'	200 bp
	Mal_r 262730075	5'- GTTCCACGAGATCCACTGGT-3'	
Peroxidase: AGAP029194	Perox_f 262730080	5'-TCTTATGCTGAGTGCCATCG-3'	190 bp
	Perox_r 262730081	5'- GTTCAGCTCCGTTATGGAA -3'	
Sage: AGAP013335	Sage_f 260891 319	5'- ATCCCGGTCAGTGTGCTAAA -3'	150 bp
	Sage_r 260891 320	5'- GAAAGCTCAGCATACCGTCC -3'	
SG6: AGAP000150	Sg6_f 260891 343	5'-TTCAAAGGCGAACGGTTCTG-3'	245 bp
	Sg6_r 260891 344	5'- GTCTCCCAGAAACGGTAGCT -3'	
Saglin: AGAP000610	Sagl_f 260891355	5'- GCAGTTTGACATTTGCGAGC -3'	150 bp
	Sagl_r 260891356	5'-ATGATGGTGAAGGTTTGCG -3'	
Actin: AGAP000651	HK_Act_f	5'-TACAACCTCGATCATGAAGTGCGA -3'	101 bp
	HK_Act_r	5'-CCC GGGTACATGGTGGTACCGCCGGA -3'	
Elongation Factor: AGAP005128	HK_EFact_f	5'-GGCAAGAGGCATAACGATCAATGCG -3'	90 bp
	HK_EFact_r	5'-GTCCATCTGCGACGCTCCGG -3'	